Identification of an epigenetic classification for hepatocellular carcinoma and biological relevance with cancer cells

Yunong Fu
The First Affiliated Hospital of Xi'an Jiaotong University
Kaibo Yang
The First Affiliated Hospital of Xi'an Jiaotong University
Kunjin Wu
The First Affiliated Hospital of Xi'an Jiaotong University
Hai Wang
The First Affiliated Hospital of Xi'an Jiaotong University
Qinglin Li
The First Affiliated Hospital of Xi'an Jiaotong University
Fengping Zhang
The First Affiliated Hospital of Xi'an Jiaotong University
Kun Yang
The First Affiliated Hospital of Xi'an Jiaotong University
Qing Yao
The First Affiliated Hospital of Xi'an Jiaotong University
Xiaohua Ma
The First Affiliated Hospital of Xi'an Jiaotong University
Yujie Deng
Xijing Hospital, Fourth Military Medical University
Jingyao Zhang
The First Affiliated Hospital of Xi'an Jiaotong University
Chang Liu
The First Affiliated Hospital of Xi'an Jiaotong University
Kai Qu (joanne8601@163.com)
The First Affiliated Hospital of Xi'an Jiaotong University

Research Article

Keywords: Hepatocellular carcinoma, Polycomb group proteins, cancer subtype, chemotherapy sensitivity, cell metabolism.

Posted Date: May 17th, 2022

DOI: https://doi.org/10.21203/rs.3.rs-1650251/v1

Abstract

Background: Hepatocellular carcinoma (HCC) is an extensive heterogeneous disease where epigenetic factors contribute to its pathogenesis. Polycomb group (PcG) proteins are a group of subunits constituting various macro molecular machines to regulate the epigenetic landscape, which contribute to cancer phenotype and have potential to develop molecular classification of HCC.

Results: Here, based on multi-omics data analysis of DNA methylation, mRNA expression and copy number of PcG-related genes, we established an epigenetic classification system of HCC, which divides the HCC patients into two subgroups with a significantly different outcome. Comparing these two epigenetic subgroups, we identified different metabolic features, which were related to epigenetic regulation of Polycomb Repressive Complex 1/2 (PRC1/2). Furthermore, we experimentally proved that inhibition of PcG complexes enhanced lipid metabolism and reduced the capacity of HCC cells against glucose shortage. In addition, we validated the low chemotherapy sensitivity of HCC in Group A, and found inhibition of PRC1/2 promoted HCC cells sensitivity to oxaliplatin *in vitro* and *in vivo*. Finally, we found that aberrant upregulation CBX2 in Group A and upregulation of CBX2 was associated with poor prognosis in HCC patients. Furthermore, we found manipulation of CBX2 affected the levels of H3K27me3 and H2AK119ub.

Conclusions: Our study provided a novel molecular classification system based on PcG-related genes data, and experimentally validated the biological features of HCC in two subgroups. Our founding supported the polycomb complex targeting strategy to inhibit HCC progression where CBX2 could be a feasible therapeutic target.

Background

Hepatocellular carcinoma (HCC) is one of the most common digestive malignancies in the world [1]. HCC is widely accepted to have heterogeneous genomic profiles contributing to its complexity in diagnosis and management [2]. There is an urgent need to employ integrative multi-omics profiling data to elucidate hepatocarcinogenesis and to identify molecular mechanisms underlying the complex clinical features of HCC [3].

Epigenetic alteration is expected to make a significant contribution to heterogeneous features of HCC. Accumulating evidence indicate that polycomb Group (PcG) complexes are the master epigenetic regulators which conduct transcriptional repression of target genes via modifying the chromatin [4]. In general, PcG complexes are divided into four types, including Polycomb Repressive Complex1/ 2 (PRC1/2), Polycomb-Repressive Deubiquitylase (PR-DUB) and Pho-repressive complex (PhoRC), to control different modification of histone in nucleus [5–8]. To constituting PcG complexes, numerous PcG subunits physically associate each other in a dynamical manner, and form a complicated molecular network in cellular process [9–11]. Furthermore, the crosstalk between different types of PcG complex,

such as hierarchical recruitment model coordinated by PRC1 and PRC2, which develops another dimension to enrich interaction pattern of PcG protein [12].

Recently, the alteration of PcG proteins has been linked to tumorigenesis and metastasis [13–15]. In mechanism, aberrant expression of PcG protein coding genes, driving by their methylation and/or copy number variation (CNV), could affect function of PcG complex and provide epigenetic perquisite for malignant transformation [16–18]. However, few study takes all of these aspects (mRNA expression, DNA methylation and gene copy number variation) into consideration when refers to influence of PcG proteins to initiation and progression of cancer. All these intrigues us to analyses the whole PcG proteins an integrity and study downstream alteration in gene expression and global phenotype.

Here, we systemically incorporated DNA methylation, mRNA expression and CNV profiling of PcG protein coding genes (PcG genes) from HCC database. Based on the multi-omics analysis, we concluded different subtypes with distinct phenotypes. Meanwhile, we analyzed the relation between those subtypes and patients' clinical features and outcomes. Experimentally, we explored the key molecule whose aberrant expression results in different HCC subtypes. In summary, we developed a novel classification based on PcG genes which has potential prognostic and therapeutic value for HCC patients.

Materials And Methods

Patient tissues obtaining

A total of 56 HCC tissues were obtained from patients who received liver biopsy partial hepatectomy or liver transplantation at First Affiliated Hospital of Xi'an Jiaotong University, and pathological data were obtained from the pathology department. Follow-up data within 5 years were collected and survival analysis was conducted through Kaplan-Meier analysis with a Log-rank test. Ethical approval was obtained from the ethics committee of First Affiliated Hospital, and informed consent was obtained from each patient.

Data collection and analysis, establishment of subtype model and other bioinformatics methods.

Gene expression data, DNA methylation data, and copy number data were obtained from UCSC Xena public database in a standard format. After patient code and gene ID matching, 372 patients with mRNA expression data of 447 PcG-related genes, DNA methylation data of 1109 PcG-related genes, and copy number data of 429 PcG-related genes were incorporated into subtype analysis. CancerSubtypes (version 1.8.0) was used to establish multi-omics HCC subtypes. Three clustering analyses (Consensus Clustering, CC, Similarity Network Fusion, SNF, and Non-negative Matrix Factorization, NFM) were performed and the optimal clustering number was chosen according to the average silhouette value. Gene set variation analysis (GSVA) and oncoplot analysis were performed by GSVA (version 1.42.0) and maftools (version 2.10.05) on R software (version 3.5.1).

Immunohistochemistry assay (IHC)

HCC tissues from patients and subcutaneous tumors from nude mice were fixed in 4% paraformaldehyde for at least 48 hours followed by dehydration and embedding in paraffin. Tissues were cut into sections for immunohistochemistry analysis. After deparaffinization with xylene, sections were subjected to antigen repair twice for 15 minutes at 100°C with an interval cooling at room temperature for 5 minutes in citrate buffer (pH = 6.0). Tissue sections were blocked by 10% goat serum (Sigma-Aldrich) for 30 minutes and incubated with appropriately diluted primary antibody overnight at 4°C (Table S1). After being washed with PBS 3 times, tissue sections were incubated with the avidin-biotin complex for 20 minutes and were developed with diaminobenzidine. Finally, the tissue sections were counterstained with hematoxylin and mounted for observation. The proportion of High Positive (HP), Positive (P), Low Positive (LP), and Negative cells were measured by the IHC profiler in Image J software (version 1.8.0). IHC scores were calculated by “IHC score = 300×HP proportion + 200×P proportion + 100× LP proportion”.

Cell culture and treatment

Human HCC cell lines (MHCC-97L and Huh7) were purchased from the Culture Collection of the Chinese Academy of Sciences (Shanghai, China). Cells were maintained in DMEM medium supplemented with 10% fetal bovine serum, 100U/mL penicillin, and 100μg/mL streptomycin to prevent contamination. Cells were cultured at 37°C in a humidified atmosphere with 5% CO2. Oxaliplatin (HY-17371, MedChemExpress), GSK126 (HY-19817, MedChemExpress), and PRT4165 (HY-19817, MedChemExpress) were dissolved in PBS or DMEM and diluted to an appropriate concentration when used.

For glucose deprivation treatment, HCC cells were seeded into 96-well plates and were maintained in a standard medium. After cell adhesion, the standard medium was replaced by a glucose-free culture medium with the palmitic acid supplement or not (10μM). After 24 hours of culture, cell viability was measured by CCK-8 assay.

RNA isolation, primer design and quantitative reverse transcription–polymerase chain reaction (qRT-PCR)

Total RNA from cells and patient tissues was extracted using Trizol (Invitrogen). Reverse transcription was performed according to the PrimeScript RT Master Mix protocol (TaKaRa, Mountain View, USA). Primers were designed using Primer-BLAST (NCBI) and were synthesized by GenePharma (Shang Hai, China). The primer sequences are shown in Table S1. TB Green Premix Ex Taq (TaKaRa) was used to perform qPCR. The β-actin (ACTB) gene was used as the internal control.

Western blot

Total protein was extracted from tissues and cells by radio immunoprecipitation assay (RIPA) lysis buffer (Beyotime). After concentration determination by BCA Protein Assay Kit (Beyotime), the protein was mixed with loading buffer (Beyotime) and heated to 100°C for 10 minutes for denaturation. Protein (5μg for the internal control and 20μg for targets) was loaded into polyacrylamide gels and separated by electrophoresis. Protein was then transferred to polyvinylidene difluoride membranes. Membranes were incubated overnight at 4°C with primary antibodies diluted in 10% milk (Table S1). After being washed

three times with PBS with 1% Tween (PBST), membranes were incubated with secondary antibodies for 30 min at room temperature. The membranes were washed 3 times with PBST before chemiluminescence.

Drug Sensitivity measurement

Drug Sensitivity measurement was based on the cell viability of HCC cells treated with oxaliplatin with a concentration of 0, 0.1, 0.5, 1.0, 5.0, 10.0, and 20.0 μg/mL, which was measured by CCK-8 assay. Cells were seeded into the 96-well plate with a density of 5000/well one day before pre-treatment of GSK126 (2μM) or/and PRT4165 (10μM). After 24 hours of pre-treatment, HCC cells were washed with PBS 3 times. A total of 10 μL CCK-8 and 90 μL serum-free DMEM were added to each well, and the microplate was incubated at 37°C for 1 h. The optical density at 450 nm was read with a 96-well multi-scanner plate reader (Biotech Instruments). Cell viability was calculated by the ratio of the optical density subtraction of treated and blank wells to the optical density subtraction of untreated and blank wells.

Gene overexpression and interference

Knockdown or overexpression of CBX2 in Huh7 and MHCC-97L cell lines was achieved by small interfering RNA targeting CBX2 mRNA or overexpression plasmid. SiRNA and plasmid were designed and synthesized by GenePharma (Shanghai, China) according to a previous study and were delivered into cells by Lipofectamine 2000 (Table S1) [19].

Immunofluorescence assay and lipid visualization

For lipid visualization, HCC cells were seeded in confocal dishes, after stable adherence cells were treated by GSK126 (2μM) or PRT4165 (10μM) for 24 hours. Then, cells were stained by BODIPY (HY-125746, MedChemExpress) with concentration of 1μM at 37°C for 20 minutes and Hoechst 33342 (Beyotime) at 37°C for 5 minutes before observation by microscope. Particle analysis was performed by Images J software (version 1.8.0).

Cell apoptosis measurement

Cell apoptosis was measured by flow cytometry analysis. HCC cells were seeded into 6-well plates and pretreated with GSK126 (2μM), PRT4165 (10μM), or together before being treated with 5μg/mL oxaliplatin. After 24 hours of oxaliplatin treatment, HCC cells were harvested with PBS three times. Then, HCC cells were stained with Annexin V-PE and 7-aminoactinomycin D (7AAD, BD) according to the manufacturer protocol and analyzed for fluorescenceusing a flow cytometer (FACSCalibur, BD). The proportion of Annexin V-PE positive cells was used to indicate the cell apoptosis rate.

Fatty acid oxidation measurement

Fatty acid oxidation measurement assay was based on the Fatty Acid Oxidation Assay (ab217602, Abcam, USA) and Extracellular Oxygen Consumption Assay (ab197243, Abcam, USA) according manufacture protocol. HCC cells were seeded into 96-well plates and were maintained in standard medium overnight. After adherence, cells were pre-treated by GSK126 (2μM) or PRT4165 (10μM) and

were maintained in glucose-deprivation (glucose-free) medium for 24 hours. Then, cells were gently washed with fatty acid-free medium. Pre-warmed fatty acid measurement medium and extracellular O2 consumption reagent was added and wells were sealed by oil. The optical signal was measure after 60 and 120 minutes by multi-scanner plate reader. Fatty acid oxidation effect was calculated by signal ratio of negative control group with inhibitor-treated group subtracted by background of blank well.

In vivo studies

Athymic nude mice were purchased from the Laboratory of Animal Research Center of Xi'an Jiaotong University. The xenograft tumor model was established in mice by subcutaneous inoculation with $1x10^6$ Huh7 cells. The oxaliplatin administration was set on the 20th day after inoculation of HCC cells (5mg/kg). On the 30th day, the mice were sacrificed and the tumors were harvested, weighed, and photographed. The protocol of animal experiments was approved by the Institutional of Animal Care and Use Committee at Xi'an Jiaotong University. The tumor volume was calculated by the formula: $V = Length \times Width^2 \times 0.5$.

Statistical analysis

All analyses were performed based on Graph Pad Prism (Version 8.0). Data represent mean ± SD from 3 repeated experiments. The student's t-test was used for comparing quantitative data. One-Way ANOVA was used for testing differences across quantitative data of multiple groups. The ranked data were analyzed with the chi-square test. Pearson correlation analyses were performed to analyze the correlation of gene expression.

Results

Identification of two epigenetic subtypes of HCC based on PcG-related genes

Accumulating evidence suggests that besides core subunits like EZH2 and BMI1, numerous accessary proteins participate in formation of PcG complexes, significantly affecting PcG complexes` function [20, 21]. To obtain the global view of PcG network in HCC, we firstly summarized a total of 448 genes (PcG-related genes) which were reported to associate with core PcG proteins [22] (Fig. 1A). Combining the RNA sequencing, DNA methylation and CNV information of these 448 PcG-related genes, we then performed multi-omics analysis and identified two novel subtypes of HCC (Group A and B) (Fig. 1B). The two subtypes had distinct clinical outcomes and patients in Group A had a worse prognosis (Fig. 1C). Moreover, a higher proportion of advanced stage and malignant phenotype was shown in Group A (Fig. 1D). Subgroup analysis showed that the prognostic differences of two subtypes were more significant in male, younger, non-Caucasian patients with advanced HCC (Fig. 1E). Above results indicated epigenetic subtype based on PcG-related Gene could predict the survival of HCC patients and reflected the biological characteristic of HCC cells.

In addition, we estimated the profile of tumor immune microenvironment in two subtypes. We found that HCC tissues of Group A exhibited a lower infiltration of NKT cells, neutrophil and endothelial cells, and a higher infiltration of B and Treg cells, consistent with their higher stroma and microenvironment scores (Fig. S1). These results indicated Group A presented an immunosuppressive and non-inflammatory microenvironment. Meanwhile, we also analyzed mutation data in different subtypes and found that the hotspot mutations mainly enriched in Wnt/β-catenin pathway member genes in Group A, while enriched in genes associated with genome integrity like *TP53* in Group B (Fig. S2). Intriguing, we also found several HCC tissues in Group A exhibited extremely higher tumor mutation burden, which indicated epigenetic subtype could affected mutation.

Two epigenetic subtypes had discrepant metabolic signatures

To further investigate the underlying molecular and biological discrepancy of two subgroups, we performed transcriptome sequencing analysis using GSVA method. Multiple signaling pathways were involved in the varying clinical characteristics of two subgroups, including inflammatory, DNA damage and repair, radiosensitivity and especially cell metabolism pathways (Fig. 2A). Group A exhibited higher level of glycolysis activity, while lower fatty acid metabolism activity. We then detected the expression of fatty acid oxidation-related genes (FAORGs) in different subtypes. We found most of FAORGs were downexpressed in Group A while overexpressed in Group B (Fig. 2B). Meanwhile, glycolysis-related genes exhibited inverse expression pattern in two groups (Fig. S3A). Intriguingly, correlation analysis showed that the expression of most FAORGs were negatively associated with PRC1/2 subunits genes, which indicated that these genes were epigenetic suppressed in Group A HCC patients (Fig. S3B). To validate this mechanism, we used PRT4165 and GSK126 to inhibit PRC1 and PRC2 activity, which decreased H3K27me3 and H2AK119ub deposition respectively (Fig. 2C). We found that PRC1/2 inhibition restored FAORGs expression (e.g., *MCEE*, *ECSH1* and *DECR1*) (Fig. 2D). These results indicated two HCC subtypes had discrepant metabolic signatures, especially in lipid and glycolytic metabolism pathways, which were affected by the activity of PcG complex.

Modulation of PcG activity affected metabolic signatures of HCC cells

To further validate the effect of the PcG activity on fatty acid metabolism, we detected the deposition of lipid droplet in HCC cells after modulating the activity of PcG complex. We found that PRC1/2 inhibitors could remarkably promoted lipid accumulation in HCC cells (Fig. 3A). Then, we measured the activity of fatty acid oxidation in HCC cells under PRC1/2 inhibitors treatment, and found that both GSK126 and PRT4165 efficiently strengthened the lipid catabolism within 120 minutes (Fig. 3B). Meanwhile, we also investigated the influence of PRC1/2 inhibition on cell viability under energy stress. We found that glucose deprivation significantly inhibited cell viability under treatment of PRC1/2 inhibitors (Fig. 3C). In contrast, palmitic acid supplement restored the synthetic lethal effect of PRC1/2 inhibition and glucose shortage (Fig. 3C). Above results supported that modulation of PcG activity induced metabolic

reprogramming of HCC cells, leading them addict to lipid metabolism but more fragile under glucose shortage, and consequently affecting tumor progression.

Inhibition of PcG complex sensitizes HCC cells to chemotherapy

The GSVA results predicted that the patients in Group A whom bearing overexpressed DNA repair-related genes, had a higher sensitivity to chemotherapy. We then investigated the effect of PcG complex inhibition on platinum-based drugs. Here, we treated HCC cells with oxaliplatin, a widely used chemotherapeutic drug for HCC [23]. We found that treatment of PRT4165 and/or GSK126 sensitized HCC cells to oxaliplatin (Fig. 4A). In addition, we detected cell apoptosis after combination treatment of PRC1/2 inhibitors and oxaliplatin (5μg/ml), and found PRC1/2 inhibitors enhanced cell sensitivity to oxaliplatin treatment and resulted in a higher proportion of cell apoptosis (Fig. 4B). Furthermore, we validated above findings *in vivo*. After 10-days' course of combination (oxaliplatin + PRC1/2 inhibitors) or single oxaliplatin treatment, we found the combination group had significantly smaller volumes and weights than single oxaliplatin treatment group (Fig. 4C). Moreover, we compared the expression of γH2A.X (a biomarker for chemotherapy-induced DNA damage) and Ki67 (a biomarker for cell proliferation) between two treatment groups and found that combination treatment group had higher γH2A.X and lower Ki67 expression than single oxaliplatin treatment group (Fig. 4D). Taken together, our data showed that inhibition of PcG complexes enhanced HCC cell sensitivity to oxaliplatin.

Overexpression of CBX2 contributed to aberrant epigenetic phenotype of HCC cells

We then investigated the molecular mechanism of epigenetic subtype. We compared the expression of PcG gene in two HCC subtype and found that CBX family coding genes (*CBX2*, *CBX4*, *CBX6* and *CBX8*) and *EZH2* were upregulated in Group A (Fig. 5A). Through survival analysis, we found that CBX2 expression is a poor prognostic factor for HCC patients (Fig. 5B). We also identified upregulation of CBX2 in cancer tissues and its association with HCC stage (Fig. 5C and S4). Previous research proved that CBX2 could mediate the crosstalk between PRC1 and PRC2 and facilitate H3K27me3 and H2AK119ub deposition [24]. Therefore, we reasoned that CBX2 overexpression might be responsible for excessive epigenetic modulation and result in aberrant epigenetic phenotype. We measured the expression of CBX2, H3K27me3 and H2AK119ub in HCC tissues using immunohistochemistry stains (Fig. 5D). We found both H3K27me3 and H2AK119ub were significantly positively correlated with CBX2 expression (Fig. 5E). In HCC cells, both of H3K27me3 and H2AK119ub were shown to be upregulated after overexpressing CBX2, and both of them were then downregulated after CBX2 inhibition (Fig. 5F, G and S5). In summary, we proved that CBX2 was a crucial contributor for aberrant epigenetic phenotypes in HCC cells and was associated with HCC epigenetic classification.

Discussion

It is well-established that aberrant expression of core PcG subunits contributes to tumor initiation and progression. In HCC, overexpression of EZH2 represses miR-622 through H3K27me3 deposition and results in CXCR4 upregulation and unfavorable prognosis, while BMI1 enhances TGFβ2/SMAD pathway and facilitates tumor cell proliferation and cell cycle progression [25, 26]. In recent years, accumulating evidence suggested that other non-core accessory proteins alternatively constituting the PcG complex can also facilitate the pro-tumor process. For example, euchromatic histone lysine methyltransferase 2 (EHMT2), an alternative subunit of PRC1.6.has been recently reported to facilitate HCC progression and aggressive features through epigenetic silencing of tumor suppressor genes [27]. In addition, although PR-DUB and PhoRC are scarcely reported in the field of HCC study, based on their close relationship with PRC1/2, we supposed that they are also functional in the epigenetic classification of HCC [28]. Therefore, in this study, aiming to analyze the subtype of HCC from the perspective of epigenetic regulation of the PcG complex in a more comprehensive picture, we included all the core and non-core proteins of four PcG complexes. Patient in two subgroups has a significantly distinct prognosis and exhibit different biological features, which is related to aberrant PcG complex activity and epigenetic landscape.

Abnormal histone modifications, especially methylation and ubiquitination, are associated with poor prognosis of cancer patients and decides biological phenotypes of tumor tissue [29–31]. It has been reported that histone methylation is associated with various malignant features like vascular invasion, large tumor size, multiplicity as well as relapse, and a previous research has also proved the tumor-promoting role of histone ubiquitination in HCC [32, 33]. For HCC, aberrant expression of PcG proteins like BMI1, CBX8, and EZH2, is mainly responsible for the deposition and maintenance of pro-tumor histone modification [26, 34]. In our study, we identified two subtypes of HCC by the analysis of the expression pattern of PcG-related genes, and CBX8 and EZH2 are upregulation in group A. Thus, we referred that Group A HCC had elevated histone methylation and ubiquitination. According to survival analysis, patients in group A have a worse prognosis, especially in young and stage □/□ subpopulation. These results suggest that the poor prognosis of Group A patients is related to pro-tumor histone modification which is consistent with previous studies.

According to our informatics analysis, HCC cells in two subgroups have distinct characteristics in many aspects, especially cell metabolism. We found that patients in Group A have lower expression of the fatty acid metabolism gene, and the downregulation of these genes can be abolished by the PRC1/2 inhibitors. Consistently, the capacity of fatty oxidation and accumulation of HCC cells were also promoted after PRC1/2 inhibitors treatment. In addition, our results showed the increased dependence on lipid and sensitivity to glucose deprivation of PRC1/2- inhibited HCC cells. In recent years, many studies have suggested that metabolic homeostasis is crucial for HCC cells in a setting of reduced nutrient availability, which can be affected by the epigenetic regulation [35–37]. Recently, Li et al proved that the deficiency of SET domain-containing 2 (SETD2), a histone methyltransferase, could cause downregulation of H3K36me3 and cholesterol efflux genes, which led to lipid accumulation and HCC development [35]. In our study, we focused on H3K27me3 and H2AK119ub which are regulated by PcG complexes, and found these histone modifications have a broad influence on the aspect of fatty acid metabolism. Intriguingly, downregulation of H3K27me3 and H2AK119ub alters HCC cells` preference of energy source from

glucose towards fatty acid and make them more fragile under the shortage of glucose, which impairs their capacity of metabolic adaption. However, whether epigenetic regulation of metabolic adaption could affect the initiation and progression of HCC needs further investigation.

The drugs targeting mutant PcG proteins such as EZH2 have been extensively investigated, and several of them have been applied to preclinical research of hematological malignancy treatment [38, 39]. However, in solid tumors, aberrant function and excessive enzymatic activity of PcG proteins are usually derived from their overexpression instead of their mutation, where the efficiency of PcG targeting drugs is limited. To solve this problem, PcG protein targeting drugs can be combined with immune therapy, conventional chemotherapy, or other targeting therapy [40, 41]. Here, we combined oxaliplatin, a widely used chemotherapeutic drug for gastrointestinal malignancy treatment, with PRC1/2 inhibitors respectively or synergistically. Our data showed that the efficiency of combined therapy to induce HCC cell apoptosis in vitro and inhibit tumor progression in vivo. In addition, our study proved that synergistic inhibition of PRC1 and PRC2 can bring higher sensitivity to oxaliplatin, and similar therapeutic strategy have recently being reported in glioblastomas treatment where the investigators successfully used molecular inhibitors of BMI1 and EZH2 to control proneural and mesenchymal tumors under the limits of detection [42]. Targeting PcG proteins dissolves the pro-tumor histone modification and enhances the sensitivity of cancer cell to other treatments.

In our study, we proved that overexpression of CBX2, the epigenetic reader, contributes to overexpression of histone methylation and ubiquitination by promoting the activity of PRC1/2 in HCC cells. As a “bridge” of PRC1 and PRC2 intercommunication, CBX2 recognizes the H3K27me3 marker and recruits other subunits of PRC1 facilitating histone modification of H2AK119ub which can be recognized by PRC2, which induces chromatin compaction for deep silence of genes [43, 44]. A previous study has reported the extranuclear function of CBX2 to activate the YAP pathway in HCC progression [19]. Here, our result showed the intranuclear function of CBX2 to promote the H3K27me3 and H2AK119ub deposition. A recent review summarized the therapeutic potential of targeting CBX2 and its advantages beyond directly targeting EZH2 [24]. Consistently, our study provided evidence that knockdown of CBX2 could simultaneously alleviate pro-cancer histone modification, and this therapeutic strategy may especially benefit HCC patients who bear an aberrant epigenetic landscape like subtype Group A patients.

Conclusions

In conclusion, our study identified a novel classification strategy of HCC patient according PcG-related gene expression and epigenetic landscape, which had significant prognostic value. Our experiment data showed the correlation between this classification system and biological features of HCC like cancer cell metabolism and chemotherapeutic sensitivity. We further found CBX2 overexpression in one subtype and proved that CBX2 could modulate epigenetic modification of histone in HCC. We proved that targeting CBX2 could be a feasible strategy to against aberrant PcG complex activity to inhibit HCC progression.

Abbreviations

HCC
Hepatocellular carcinoma
PRC1/2
Polycomb Repressive Complex 1/2
H3K27me3
Tri-Methyl-Histone H3 (Lys27)
H2AK119ub
Ubiquityl-Histone H2A (Lys119)
PR-DUB
Polycomb-Repressive Deubiquitylase
PhoRC
Pho-repressive Complex
CNV
Copy Number Variation
NFM
Non-negative Matrix Factorization
CC
Consensus Clustering
SNF
Similarity Network Fusion
GSVA
Gene Set Variation Analysis
qRT-PCR
Quantitative Reverse Transcription–polymerase Chain Reaction
FAORGs
Fatty Acid Oxidation-Related Genes
IHC
Immunohistochemistry Assay.

Declarations

Acknowledgements

We thank Yunxiang Long and Tong Liu for the experiment preparation.

Authors' contributions

Yunong Fu, Kai Qu, Chang Liu and Jingyao Zhang conceived and designed the study. Yunong Fu and Kaibo Yang conducted the bioinformatics analysis. Yunong Fu, Kaibo Yang, Kunjin Wu and Fengping Zhang performed the in vitro experiments. Yunong Fu, Qinglin Li, Xiaohua Ma and Qing Yao performed

the in vivo experiments. Kun Yang, Hai Wang and Yujie Deng provided clinical samples and performed immunohistochemical staining.

Funding

This project was funded by the National Natural Science Foundation of China (Nos. 82072145, 81871998 and 81972236) and the Natural Science Foundation of Shaanxi Province (2020JM-373).

Availability of data and materials

The datasets analyzed for the current study are available from the corresponding author on reasonable request.

Ethics approval and consent to participate

All subjects signed an informed consent form. The study was approved by the Ethics Committee of the First Affiliated Hospital of Xi'an Jiaotong University. Moreover, consent was received from each patient before their tissues are collected for research.

Consent for publication

We confirm that all authors have agreed with the submission in its present (and subsequent) forms.

Competing interests

The authors declare that they have no competing interests.

References

1. Sung, H., J. Ferlay, R.L. Siegel, et al., *Global Cancer Statistics 2020: GLOBOCAN Estimates of Incidence and Mortality Worldwide for 36 Cancers in 185 Countries*. CA Cancer J Clin, 2021. **71**(3): p. 209–249.
2. *Comprehensive and Integrative Genomic Characterization of Hepatocellular Carcinoma*. Cell, 2017. **169**(7): p. 1327–1341.e23.
3. Dong, L., D. Lu, R. Chen, et al., *Proteogenomic characterization identifies clinically relevant subgroups of intrahepatic cholangiocarcinoma*. Cancer Cell, 2022. **40**(1): p. 70–87.e15.

4. Schuettengruber, B., H.M. Bourbon, L. Di Croce, et al., *Genome Regulation by Polycomb and Trithorax: 70 Years and Counting*. Cell, 2017. **171**(1): p. 34–57.
5. Shao, Z., F. Raible, R. Mollaaghababa, et al., *Stabilization of chromatin structure by PRC1, a Polycomb complex*. Cell, 1999. **98**(1): p. 37–46.
6. Czermin, B., R. Melfi, D. McCabe, et al., *Drosophila enhancer of Zeste/ESC complexes have a histone H3 methyltransferase activity that marks chromosomal Polycomb sites*. Cell, 2002. **111**(2): p. 185–96.
7. Klymenko, T., B. Papp, W. Fischle, et al., *A Polycomb group protein complex with sequence-specific DNA-binding and selective methyl-lysine-binding activities*. Genes Dev, 2006. **20**(9): p. 1110–22.
8. Scheuermann, J.C., A.G. de Ayala Alonso, K. Oktaba, et al., *Histone H2A deubiquitinase activity of the Polycomb repressive complex PR-DUB*. Nature, 2010. **465**(7295): p. 243–7.
9. Cao, R., Y. Tsukada andY. Zhang, *Role of Bmi-1 and Ring1A in H2A ubiquitylation and Hox gene silencing*. Mol Cell, 2005. **20**(6): p. 845–54.
10. Taherbhoy, A.M., O.W. Huang andA.G. Cochran, *BMI1-RING1B is an autoinhibited RING E3 ubiquitin ligase*. Nat Commun, 2015. **6**: p. 7621.
11. Li, Z., R. Cao, M. Wang, et al., *Structure of a Bmi-1-Ring1B polycomb group ubiquitin ligase complex*. J Biol Chem, 2006. **281**(29): p. 20643–9.
12. Wang, L., J.L. Brown, R. Cao, et al., *Hierarchical recruitment of polycomb group silencing complexes*. Mol Cell, 2004. **14**(5): p. 637–46.
13. Yuan, H., Y. Han, X. Wang, et al., *SETD2 Restricts Prostate Cancer Metastasis by Integrating EZH2 and AMPK Signaling Pathways*. Cancer Cell, 2020. **38**(3): p. 350–365.e7.
14. Li, J., Y. Xu, X.D. Long, et al., *Cbx4 governs HIF-1α to potentiate angiogenesis of hepatocellular carcinoma by its SUMO E3 ligase activity*. Cancer Cell, 2014. **25**(1): p. 118–31.
15. Zhang, Y., J. Shi, X. Liu, et al., *H2A Monoubiquitination Links Glucose Availability to Epigenetic Regulation of the Endoplasmic Reticulum Stress Response and Cancer Cell Death*. Cancer Res, 2020. **80**(11): p. 2243–2256.
16. Yu, H., M. Ma, J. Yan, et al., *Identification of coexistence of BRAF V600E mutation and EZH2 gain specifically in melanoma as a promising target for combination therapy*. J Transl Med, 2017. **15**(1): p. 243.
17. Meunier, L., T.Z. Hirsch, S. Caruso, et al., DNA Methylation Signatures Reveal the Diversity of Processes Remodeling Hepatocellular Carcinoma Methylomes. Hepatology, 2021. **74**(2): p. 816–834.
18. Muir, K., A. Hazim, Y. He, et al., *Proteomic and lipidomic signatures of lipid metabolism in NASH-associated hepatocellular carcinoma*. Cancer Res, 2013. **73**(15): p. 4722–31.
19. Mao, J., Y. Tian, C. Wang, et al., *CBX2 Regulates Proliferation and Apoptosis via the Phosphorylation of YAP in Hepatocellular Carcinoma*. J Cancer, 2019. **10**(12): p. 2706–2719.
20. Wang, D., X. Li, J. Li, et al., *APOBEC3B interaction with PRC2 modulates microenvironment to promote HCC progression*. Gut, 2019. **68**(10): p. 1846–1857.

21. Xu, P., D.C. Scott, B. Xu, et al., *FBXO11-mediated proteolysis of BAHD1 relieves PRC2-dependent transcriptional repression in erythropoiesis*. Blood, 2021. **137**(2): p. 155–167.
22. Hauri, S., F. Comoglio, M. Seimiya, et al., *A High-Density Map for Navigating the Human Polycomb Complexome*. Cell Rep, 2016. **17**(2): p. 583–595.
23. Lyu, N., Y. Kong, L. Mu, et al., *Hepatic arterial infusion of oxaliplatin plus fluorouracil/leucovorin vs. sorafenib for advanced hepatocellular carcinoma*. J Hepatol, 2018. **69**(1): p. 60–69.
24. Jangal, M., B. Lebeau andM. Witcher, *Beyond EZH2: is the polycomb protein CBX2 an emerging target for anti-cancer therapy?* Expert Opin Ther Targets, 2019. **23**(7): p. 565–578.
25. Li, B., Y. Chen, F. Wang, et al., *Bmi1 drives hepatocarcinogenesis by repressing the TGFβ2/SMAD signalling axis*. Oncogene, 2020. **39**(5): p. 1063–1079.
26. Liu, H., Y. Liu, W. Liu, et al., *EZH2-mediated loss of miR-622 determines CXCR4 activation in hepatocellular carcinoma*. Nat Commun, 2015. **6**: p. 8494.
27. Wei, L., D.K. Chiu, F.H. Tsang, et al., *Histone methyltransferase G9a promotes liver cancer development by epigenetic silencing of tumor suppressor gene RARRES3*. J Hepatol, 2017. **67**(4): p. 758–769.
28. Frey, F., T. Sheahan, K. Finkl, et al., *Molecular basis of PRC1 targeting to Polycomb response elements by PhoRC*. Genes Dev, 2016. **30**(9): p. 1116–27.
29. Jeusset, L.M. andK.J. McManus, *Developing Targeted Therapies That Exploit Aberrant Histone Ubiquitination in Cancer*. Cells, 2019. **8**(2).
30. Michalak, E.M., M.L. Burr, A.J. Bannister, et al., *The roles of DNA, RNA and histone methylation in ageing and cancer*. Nat Rev Mol Cell Biol, 2019. **20**(10): p. 573–589.
31. Füllgrabe, J., E. Kavanagh andB. Joseph, Histone onco-modifications. Oncogene, 2011. **30**(31): p. 3391–403.
32. Cai, M.Y., J.H. Hou, H.L. Rao, et al., *High expression of H3K27me3 in human hepatocellular carcinomas correlates closely with vascular invasion and predicts worse prognosis in patients*. Mol Med, 2011. **17**(1–2): p. 12–20.
33. Xu, L., J. Lin, W. Deng, et al., *EZH2 facilitates BMI1-dependent hepatocarcinogenesis through epigenetically silencing microRNA-200c*. Oncogenesis, 2020. **9**(11): p. 101.
34. Tang, B., Y. Tian, Y. Liao, et al., *CBX8 exhibits oncogenic properties and serves as a prognostic factor in hepatocellular carcinoma*. Cell Death Dis, 2019. **10**(2): p. 52.
35. Li, X.J., Q.L. Li, L.G. Ju, et al., *Deficiency of Histone Methyltransferase SET Domain-Containing 2 in Liver Leads to Abnormal Lipid Metabolism and HCC*. Hepatology, 2021. **73**(5): p. 1797–1815.
36. Puszyk, W.M., T.L. Trinh, S.J. Chapple, et al., *Linking metabolism and epigenetic regulation in development of hepatocellular carcinoma*. Lab Invest, 2013. **93**(9): p. 983–90.
37. Shang, R.Z., S.B. Qu andD.S. Wang, *Reprogramming of glucose metabolism in hepatocellular carcinoma: Progress and prospects*. World J Gastroenterol, 2016. **22**(45): p. 9933–9943.

38. Duan, R., W. Du andW. Guo, *EZH2: a novel target for cancer treatment*. J Hematol Oncol, 2020. **13**(1): p. 104.
39. Seipel, K., B. Kopp, U. Bacher, et al., *BMI1-Inhibitor PTC596 in Combination with MCL1 Inhibitor S63845 or MEK Inhibitor Trametinib in the Treatment of Acute Leukemia*. Cancers (Basel), 2021. **13**(3).
40. Gounder, M., P. Schöffski, R.L. Jones, et al., *Tazemetostat in advanced epithelioid sarcoma with loss of INI1/SMARCB1: an international, open-label, phase 2 basket study*. Lancet Oncol, 2020. **21**(11): p. 1423–1432.
41. Zhou, L., T. Mudianto, X. Ma, et al., *Targeting EZH2 Enhances Antigen Presentation, Antitumor Immunity, and Circumvents Anti-PD-1 Resistance in Head and Neck Cancer*. Clin Cancer Res, 2020. **26**(1): p. 290–300.
42. Jin, X., L.J.Y. Kim, Q. Wu, et al., *Targeting glioma stem cells through combined BMI1 and EZH2 inhibition*. Nat Med, 2017. **23**(11): p. 1352–1361.
43. Kalb, R., S. Latwiel, H.I. Baymaz, et al., *Histone H2A monoubiquitination promotes histone H3 methylation in Polycomb repression*. Nat Struct Mol Biol, 2014. **21**(6): p. 569–71.
44. Tamburri, S., E. Lavarone, D. Fernández-Pérez, et al., *Histone H2AK119 Mono-Ubiquitination Is Essential for Polycomb-Mediated Transcriptional Repression*. Mol Cell, 2020. **77**(4): p. 840–856.e5.

Figures

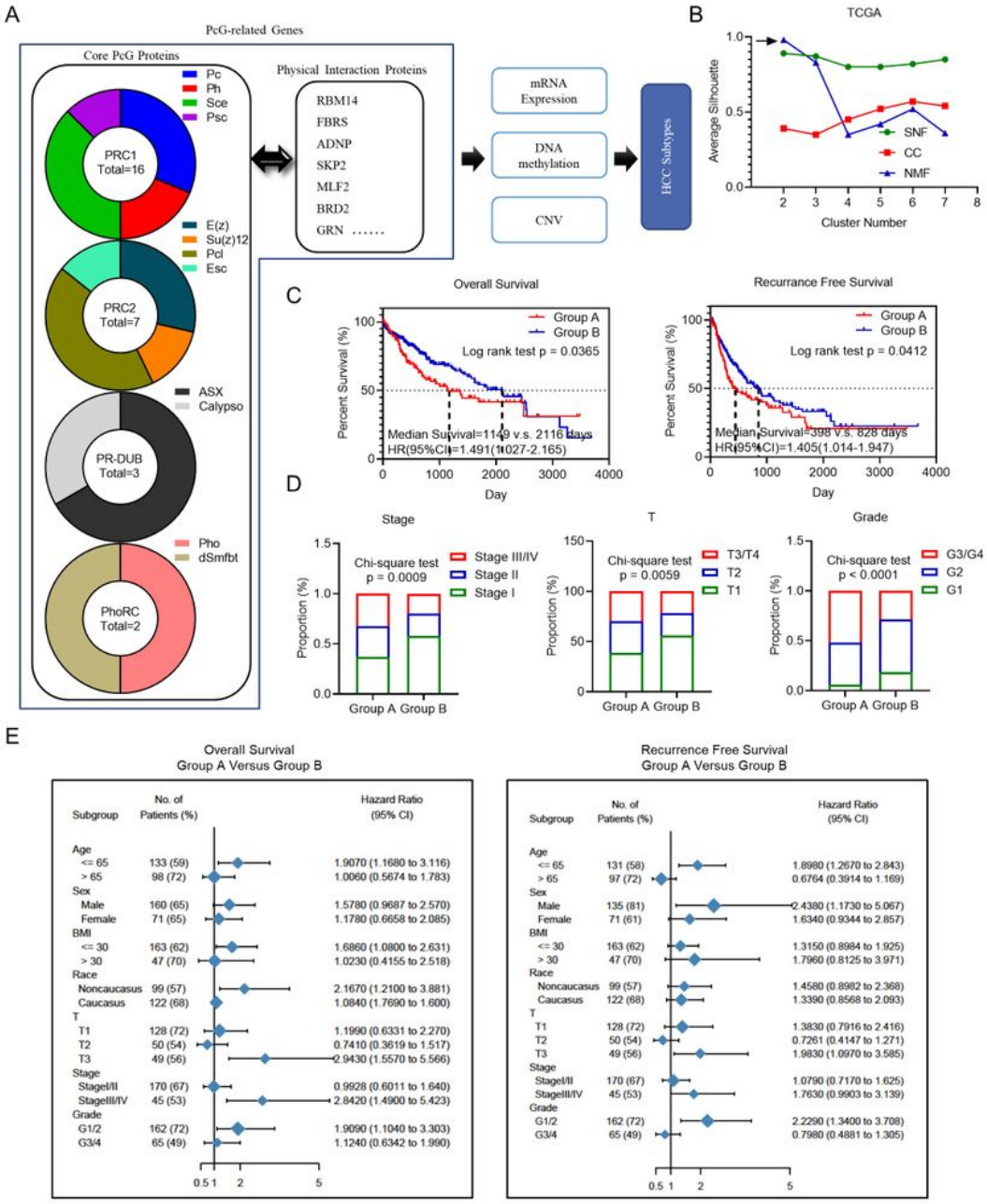

Figure 1

Identification of two epigenetic subtypes of HCC based on PcG-related genes. A. The flow diagram of establishment of epigenetic classification of HCC based on bioinformatics analysis. **B.** Average silhouette values of different clustering method and cluster number. The black arrows indicates optimized clustering strategy. **C.** Survival analysis of HCC patients in two epigenetic subtypes. **D.** Comparation of

clinicopathologic feature of HCC patients in different epigenetic subgroups. **E.** Stratification analysis of HCC patients in different epigenetic subgroups according to their clinical data.

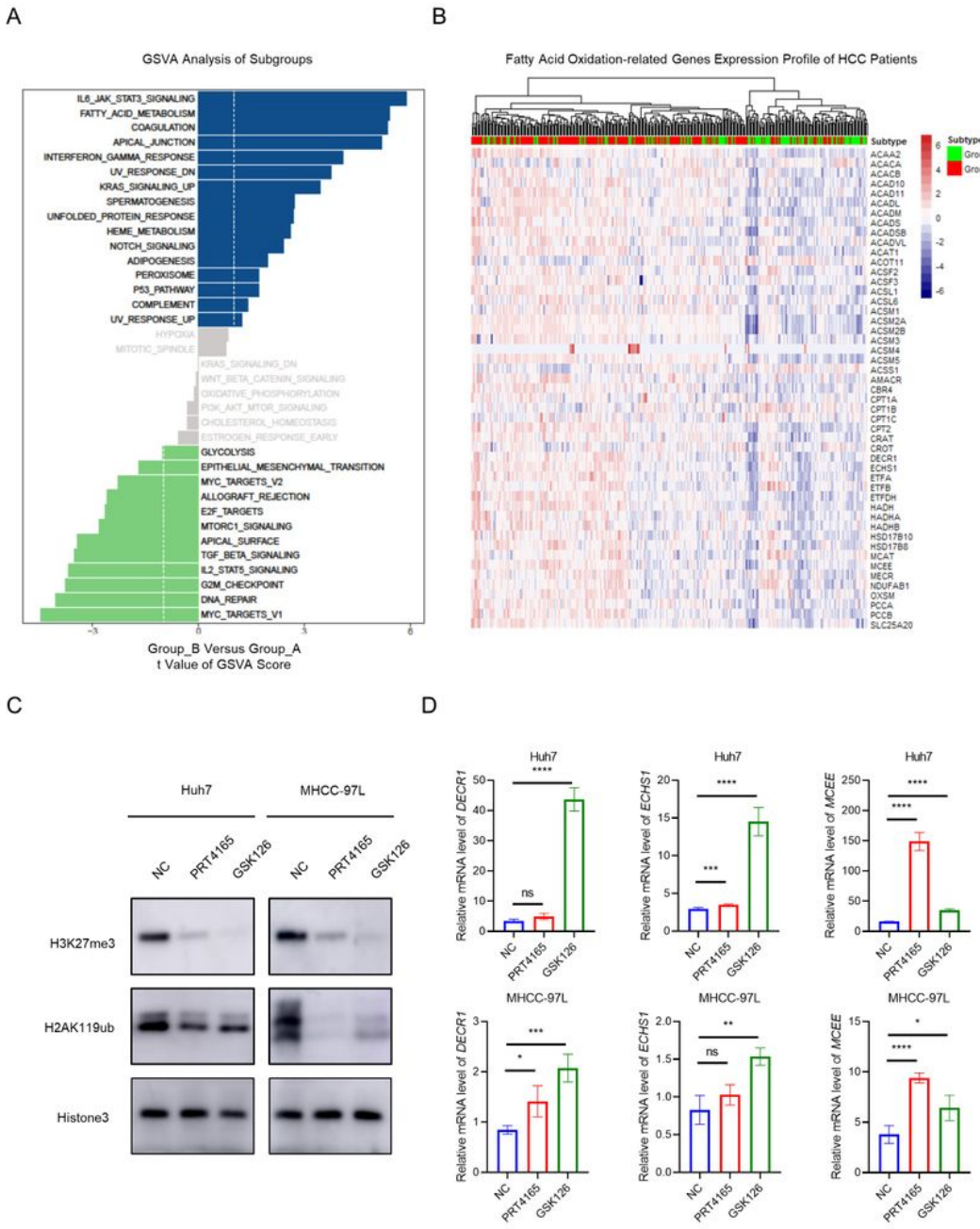

Figure 2

Two epigenetic subtypes had discrepant metabolic signatures. A. Gene Set Variation Analysis (GSVA) of mRNA expression profile in HCC of different epigenetic subgroups. **B.** Fatty acid oxidation-related genes expression profile of HCC in different epigenetic subgroups. **C.** The downregulation of H3K27me3 and H2AK119ub protein level in HCC cells after GSK126 or PRT4165 treatment. **D.** The downregulation of three fatty acid oxidation-related genes mRNA expression in HCC cells after GSK126 or PRT4165 treatment. β-actin (ACTB) was used as internal control. Ns, not significant; *, p<0.05; **, p<0.01; ***, p<0.005; ****, p<0.001.

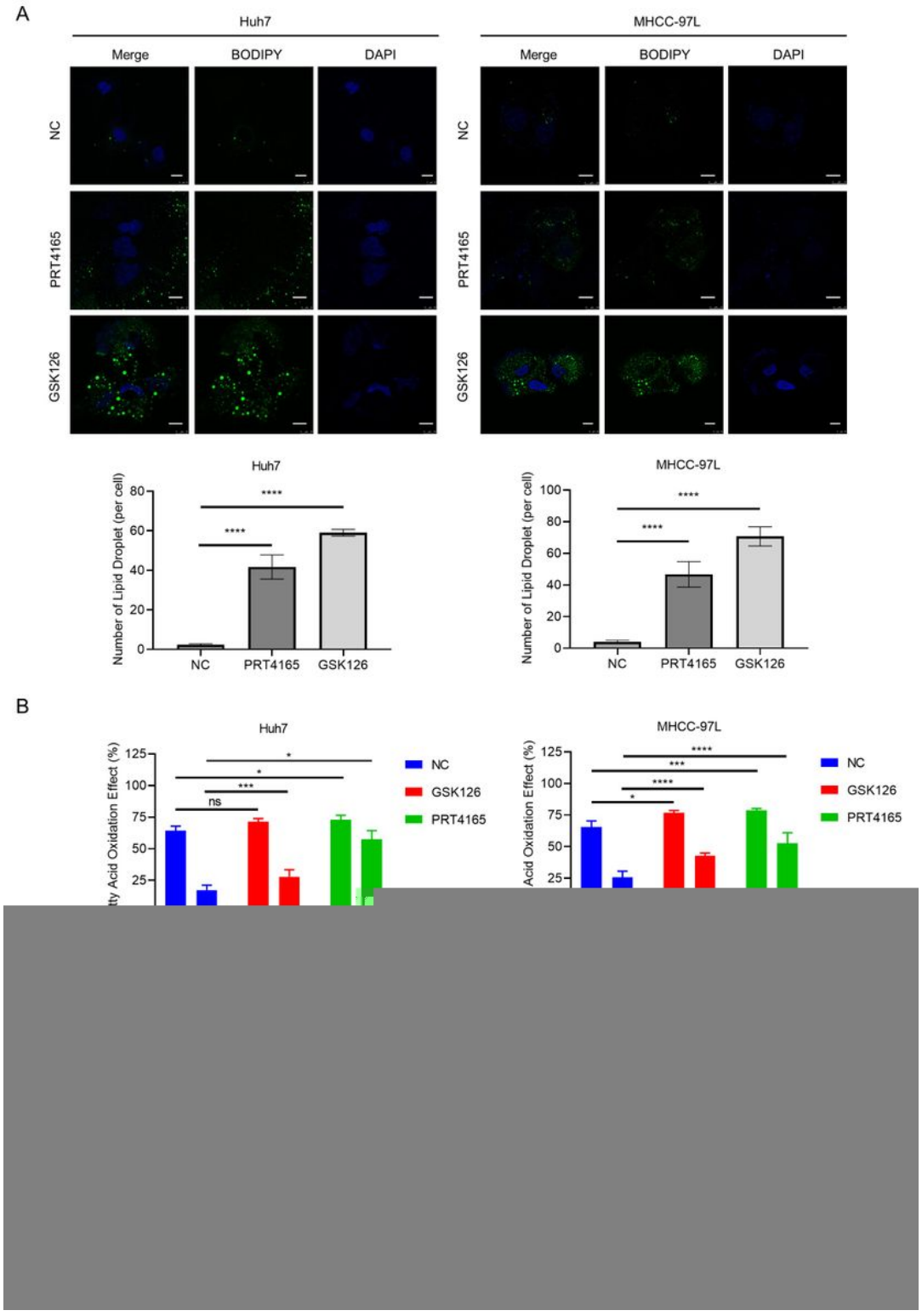

Figure 3

Modulation of PcG activity affected metabolic signatures of HCC cells. A. The lipid fluorescence staining of HCC cells after GSK126 or PRT4165 treatment. The white arrow indicated 10μm. Three independent assays were analyzed and average number of lipid droplet of each field was measured. ****, p<0.001. **B.** The fatty acid oxidation effect of HCC cell after GSK126 or PRT4165 treatment. Three independent assays were performed and data were collected at 60 and 120 minutes time points. Ns, not significant; *, p<0.05; ***, p<0.005; ****, p<0.001. **C.** Cell viability of HCC cells after glucose deprivation with or without treatment of GSK126 or PRT4165 and after supplement of palmitic acid (10μM). Three independent assays were performed. Ns, not significant; *, p<0.05; ***, p<0.005; ****, p<0.001.

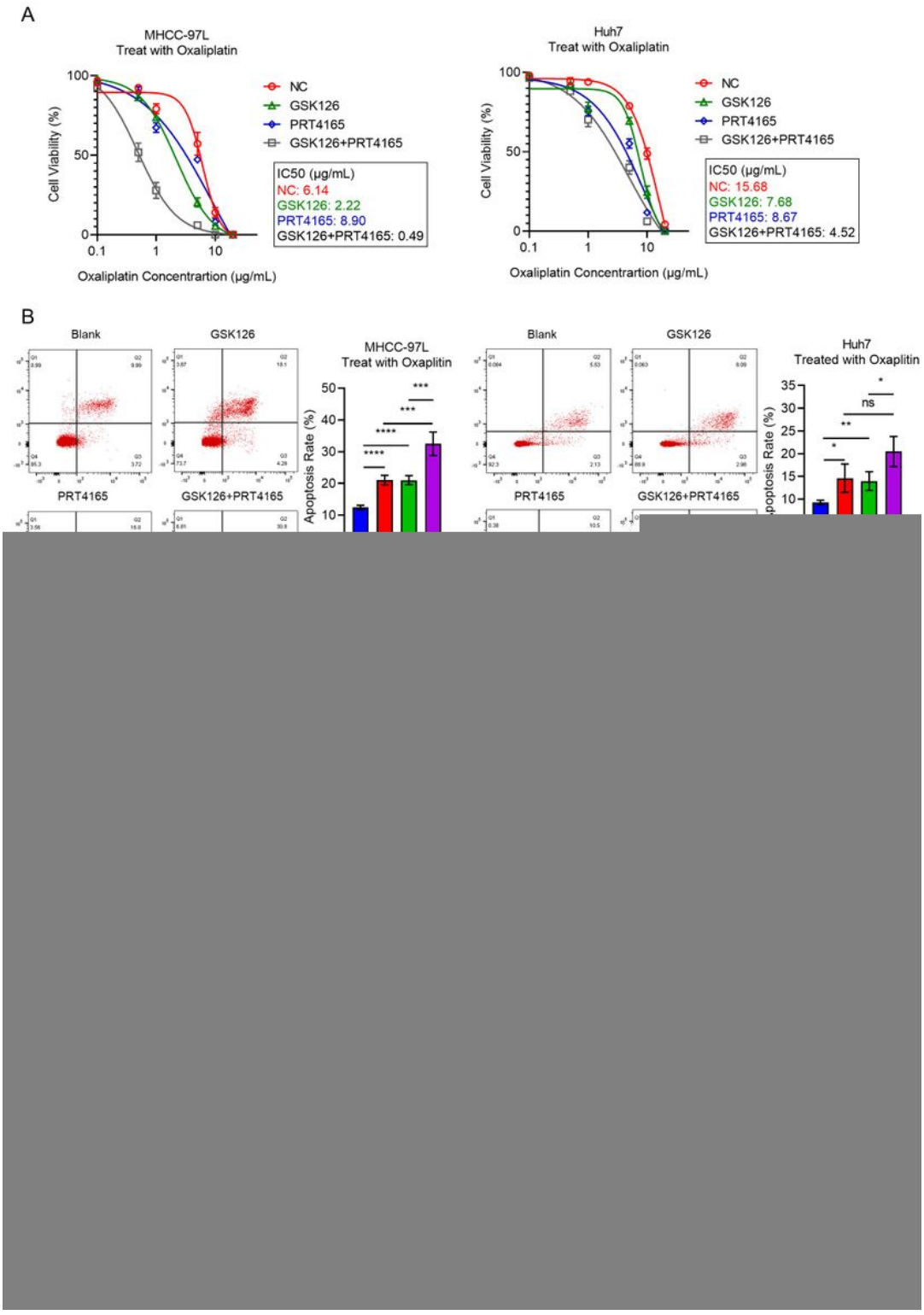

Figure 4

Inhibition of PcG complex sensitizes HCC cells to chemotherapy. A. Cell viability of HCC cells under treatment of oxaliplatin together with GSK126 or PRT4165. The signal from three independent wells were collected and 50% inhibitory concentration (IC50B) was calculated by four parameters model. **B.** Cell apoptosis rate of HCC cell after oxaliplatin treatment (5μg/ml) with GSK126 or PRT4165 measured by flow cytometry. Ns, not significant; *, p<0.05; **, p<0.01; ***, p<0.005; ****, p<0.001. **C.** Huh7-cell derived

subcutaneously tumor after treatment of oxaliplatin with or without GSK126 and PRT4165. ***, p<0.005; ****, p<0.001. **D.** The IHC assay of γH2A.X and Ki67 subcutaneously tumor after low dose oxaliplatin treatment with or without GSK126 and PRT4165. The black bar represents 100μm, and *, p<0.05; ***, p<0.005.

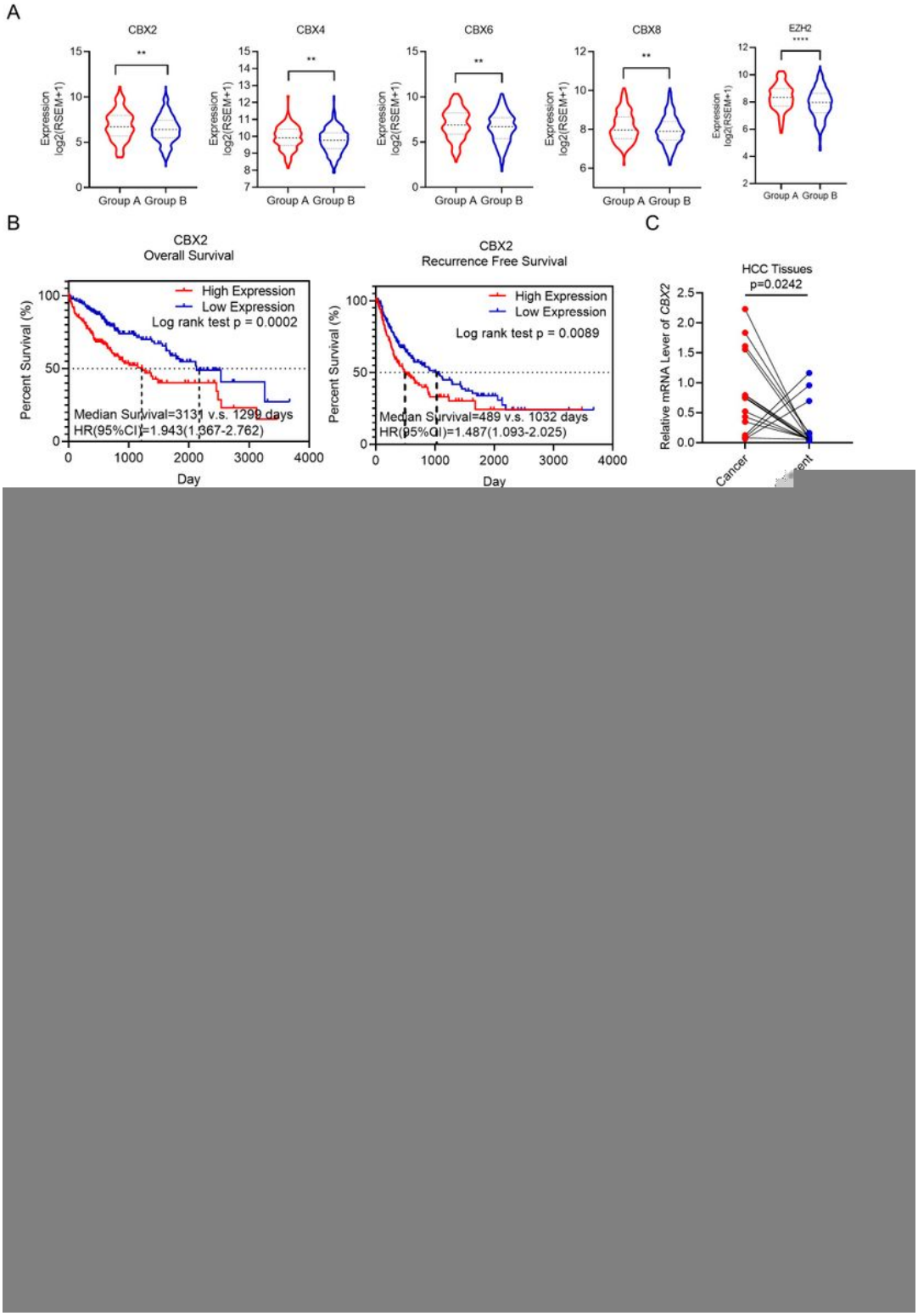

Figure 5

Overexpression of CBX2 contributes to aberrant epigenetic landscape of HCC cells. A. The mRNA expression of PcG genes of HCC patients in different epigenetic subgroups. **, p<0.01; ****, p<0.001. **B.** The Kaplan-Meier curve based on survival analysis of HCC patients expressing high or low level of CBX2. **C.** The mRNA level of CBX2 in tumor and adjacent tissue of HCC patients. The relative mRNA level were normalized by β-actin (ACTB). **D.** The IHC assay of CBX2, H3K27me1 and H2AK119ub in high and low CBX2 expression HCC groups. The black bars represent 200μm. **E.** The correlation analysis of CBX2 expression with H3K27me3 or H2AK119ub expression. The Pearson coefficients were calculated. **F.** The immunoblot of H3K27me1 and H2AK119ub in CBX2 knockdown HCC cells. **G.** The immunoblot of H3K27me3 and H2AK119ub in CBX2 overexpression HCC cells.

Supplementary Files

This is a list of supplementary files associated with this preprint. Click to download.

- FigS1.jpg
- FigS2.jpg
- FigS3.jpg
- FigS4.jpg
- FigS5.jpg